

1 Evidence for Transcriptome-wide RNA Editing Among *Sus scrofa* PRE-1

2 SINE Elements

3

4

5 Scott A. Funkhouser<sup>1</sup>, Juan P. Steibel<sup>2</sup>, Ronald O. Bates<sup>2</sup>, Nancy E. Raney<sup>2</sup>, Darius

6 Schenk<sup>3</sup>, Catherine W. Ernst<sup>2\*</sup>

7

8 <sup>1</sup> Genetics Graduate Program, Michigan State University, East Lansing, Michigan,

9 48824, United States of America

10 <sup>2</sup> Department of Animal Science, Michigan State University, East Lansing, Michigan,

11 48824, United States of America

12 <sup>3</sup> Heinrich-Heine University, Dusseldorf, Germany

13

14 \*Corresponding author: ernstc@msu.edu

15

16 E-mail:

17 funkhou9@msu.edu (SAF)

18 steibelj@msu.edu (JPS)

19 batesr2@anr.msu.edu (ROB)

20 raney@msu.edu (NER)

21 darius.schenk@gmail.com (DS)

22 ernstc@msu.edu (CWE)

23

## 24 **Abstract**

25 **Background:** RNA editing by ADAR (adenosine deaminase acting on RNA) proteins is  
26 a form of transcriptional regulation that is widespread among humans and other primates.  
27 Based on high-throughput scans used to identify putative RNA editing sites, ADAR  
28 appears to catalyze a substantial number of adenosine to inosine transitions within  
29 repetitive regions of the primate transcriptome, thereby dramatically enhancing genetic  
30 variation beyond what is encoded in the genome.

31 **Results:** Here, we demonstrate the editing potential of the pig transcriptome by utilizing  
32 DNA and RNA sequence data from the same pig. We identified a total of 8550  
33 mismatches between DNA and RNA sequences across three tissues, with 75% of these  
34 exhibiting an A-to-G (DNA to RNA) discrepancy, indicative of a canonical ADAR-  
35 catalyzed RNA editing event. When we consider only mismatches within repetitive  
36 regions of the genome, the A-to-G percentage increases to 94%, with the majority of  
37 these located within the swine specific SINE retrotransposon PRE-1. We also observe  
38 evidence of A-to-G editing within coding regions that were previously verified in  
39 primates.

40 **Conclusions:** Thus, our high-throughput evidence suggests that pervasive RNA editing  
41 by ADAR can exist outside of the primate lineage to dramatically enhance genetic  
42 variation in pigs.

43

44

## 45 **Keywords**

46 PRE-1, RNA editing, swine, bioinformatics

47

## 48 **Background**

49 Eukaryotes are known for relatively complex mechanisms used to regulate gene  
50 expression. One such mechanism, RNA editing, enables the cell to alter sequences of  
51 RNA transcripts [1] such that they are no longer forced to match the “hard-wired”  
52 genome sequence. High throughput methods for studying targets of this mechanism  
53 transcriptome-wide have been applied to primate studies, where evidence for massive  
54 amounts of ADAR (adenosine deaminase acting on RNA) catalyzed A-to-I RNA editing  
55 has been discovered, preferentially within SINE retrotransposons such as the primate Alu  
56 [2 – 8]. Such work has yet to be performed with pig transcriptomes using the latest  
57 sequencing technology. Although little is known about pig SINE elements compared to  
58 those in primates, key features of the pig-specific PRE-1 retrotransposon make pigs an  
59 intriguing model to further elucidate transcriptome-wide patterns of ADAR targets.

60 ADAR can only catalyze A-to-I editing within dsRNA. The high editability of the  
61 primate specific Alu element is attributed to its capacity to induce dsRNA; these elements  
62 have a high copy number, are short, relatively undiverged from one another, and tend to  
63 cluster in gene rich regions of the genome [9]. When appearing as tandem and inverted  
64 pairs within the same transcribed region, these properties facilitate intra-molecular  
65 dsRNA formation that serve as ADAR targets [2, 10]. Comparatively, the pig PRE-1  
66 element possesses many of these same properties that are believed to contribute to

67 dsRNA formation within the transcriptome. Notably, PRE-1 has the 3<sup>rd</sup> highest copy  
68 number of any SINE cataloged on SINEBase [11].

69         Since Alu elements are generally found within and near genes, ADAR editing in  
70 humans preferentially targets non-coding regions of many genes such as introns, UTRs  
71 and upstream and downstream gene proximal regions. ADAR editing of these regions is  
72 thought to be a key component of RNA processing via mechanisms that include Alu  
73 exonization [12] and RNAi pathway alteration [13]. By demonstrating that RNA editing  
74 in pigs generally targets SINE elements within non-coding regions of genes, this would  
75 suggest that RNA processing by way of ADAR editing of SINE elements predated the  
76 emergence of primate and pig-specific retrotransposons. Rarely, ADAR editing occurs  
77 within coding regions to alter amino acid sequences [14]. This type of editing is  
78 particularly mysterious in that its pattern is less traceable than non-coding editing, but is  
79 nevertheless site-specific and required for the function of essential protein coding genes  
80 such as *GluR-B* in mice [15]. Therefore, in addition to the regulation of transcripts by  
81 way of editing non-coding SINE elements, editing of coding regions is an essential form  
82 of transcriptional regulation in mice, with the extent of its conservation across Mammalia  
83 yet to be fully determined.

84         Here, we demonstrate the pig's capacity for RNA editing. By studying this  
85 process in a relatively distant species to human with a distinct repetitive element  
86 repertoire, we want to determine if RNA editing patterns seen in Alu bearing genomes  
87 can likewise be observed in pigs. RNA editing detection was done by analyzing a single  
88 pig using whole genome sequencing data and RNA sequencing data from liver,  
89 subcutaneous fat, and *longissimus dorsi* muscle. Based on previous studies done in

90 primates, a bioinformatic strategy was used to find A-to-I (observed as A-to-G) DNA to  
91 RNA mismatches that give evidence of ADAR catalyzed RNA editing events.

92

## 93 **Results and discussion**

### 94 **DNA and RNA sequencing**

95 To provide the materials needed for a transcriptome-wide survey of RNA editing  
96 candidates, genomic DNA as well as total RNA from liver, subcutaneous fat, and  
97 *longissimus dorsi* (LD) muscle were purified from samples obtained from a single  
98 animal, similar to another single-animal editome study [8]. Sequencing was done using  
99 the Illumina HiSeq 2500 to generate 150x2 paired end reads from genomic DNA, with  
100 PolyA RNA sequencing used to generate cDNA reads in the same format. Roughly 250M  
101 pass-filter genomic DNA reads were generated with an average overall alignment rate of  
102 89% to the *Sus scrofa* reference genome sequence (*Sus scrofa* 10.2.69). An average of  
103 106M pass-filter strand specific cDNA reads were obtained from each tissue, with an  
104 average overall alignment rate of 76%.

### 105 **Identification of candidate RNA editing events**

106 To scan the transcriptome for possible RNA editing sites, we utilized a custom  
107 pipeline influenced by previous studies done in human cell lines and primates [16, 8].  
108 Prior to alignment, in order to avoid utilizing bases with relatively poor base qualities at  
109 the ends of reads, raw genomic DNA and cDNA sequencing reads were trimmed for base  
110 quality at their 3' ends before aligning to the *Sus scrofa* 10.2.69 reference genome.  
111 Additional trimming 6bp from the 5' ends of cDNA reads was done to prevent

112 misidentification of DNA RNA mismatches due to artifacts associated with the use of  
113 random hexamers during cDNA library preparation [17]. When conducting a search for  
114 RNA editing candidates with RNA-seq, strand-specific RNA-seq libraries can be utilized  
115 to account for the strandedness of each transcript, thereby enabling A-to-G DNA-to-RNA  
116 mismatches to be distinguished from T-to-C DNA-to-RNA mismatches. In order to  
117 utilize our strand-specific cDNA alignments for variant calling while preserving the  
118 strandedness of each alignment to distinguish A-to-G from T-to-C mismatches, plus-  
119 strand alignments were separated from minus-strand alignments for each cDNA sample.  
120 From all genomic DNA and cDNA alignments, we extracted those reads that had only 1  
121 recorded alignment in order to optimize our chances that genomic DNA and cDNA reads  
122 arising from the same locus map to the same location. Joint variant calling using  
123 SAMTools [18] was performed, combining genomic DNA alignments with cDNA plus-  
124 strand alignments from each tissue. This was repeated for all cDNA minus-strand  
125 alignments. Both resulting VCF files were analyzed using editTools, an in-house R  
126 package made to efficiently scan VCF files for DNA RNA mismatches using C++ source  
127 code. editTools was developed to implement RNA editing detection within the R  
128 framework and to provide visualization tools; editTools was used to generate all figures  
129 in this manuscript pertaining to sequencing data. Default editTools parameters were used,  
130 in which a mismatch was considered a candidate RNA editing site if at a particular locus  
131 1) the genotype is homozygous according to 95% of the DNA reads, 2) at least 10 reads  
132 were used to determine the genotype, 3) neither genomic DNA nor cDNA samples are  
133 indels, 4) at least 5 cDNA reads from the same tissue differ from the genotype call, and  
134 5) these cDNA reads must have a Phred-scaled strand-bias P-value of 20 or less. Specific

135 thresholds for DNA and cDNA sequencing depths were determined according to a  
136 previous study that profiled the rhesus macaque editome from a single animal [8]. Using  
137 this approach, we identified a total of 6410 A-to-G mismatch events representing 75% of  
138 all mismatches found (8550 total mismatches; Fig. 1). When we restrict our search to  
139 known swine repetitive sequences, 5993 out of 6410 A-to-G mismatches are retained,  
140 representing 93.8% of all mismatches in repetitive regions. Of the remaining mismatches  
141 in repetitive regions, 4.1% are T-to-C. It is not surprising that T-to-C mismatches are the  
142 second most common since T-to-C artifacts could arise if at a true A-to-G editing site,  
143 plus-strand alignments were incorrectly identified as minus-strand alignments or vice  
144 versa.

## 145 **Tissue differences**

146 To understand differences in candidate RNA editing sites between tissues,  
147 canonical A-to-G mismatches were aligned across tissues if they were detected at the  
148 same physical position and on the same strand. The number of candidate RNA editing  
149 events was fewer in LD compared to liver or fat (Fig. 1), consistent with lower RNA  
150 editing activity in muscle compared to other tissues for rhesus macaque [8]. Despite  
151 candidate RNA editing sites showing strong tissue specificity, a total of 144 A-to-G  
152 mismatches were found to be common among all three tissues, whereas 748 were found  
153 to be common between liver and fat (Fig. 2).

154 One factor that may contribute to tissue specificity of RNA editing is differential  
155 expression of ADAR [19]. Using RNA samples from 33 additional pigs, a quantitative  
156 real-time PCR assay was used to infer ADAR transcript abundance differences between  
157 liver, subcutaneous fat, and LD muscle (Fig. 3). Average ADAR expression was

158 determined to be significantly lower in LD muscle tissue than in either fat ( $p < 0.0003$ ) or  
159 liver ( $p < 0.00001$ ) tissues, suggesting that differential ADAR expression may contribute  
160 to differences in candidate RNA editing sites between tissues.

## 161 **Controlling for errors due to mapping quality**

162 After imposing such strict restrictions as excluding genomic DNA and cDNA  
163 reads that had more than one recorded alignment and trimming the ends of reads pre-  
164 alignment, we wanted to assess how well such measures protect against mapping errors,  
165 which are among the leading causes of RNA editing misidentification when using short  
166 reads [17, 20]. Mapping quality is a measurement that provides a probability that a read is  
167 misaligned, given its number of possible alignments and sum of base qualities for each  
168 alignment [21]. Knowing this, and under the assumption of no RNA editing, for each  
169 mismatch locus  $i$  we computed the probability of observing at least 5 “edited” reads  
170 given the cDNA sequencing depth  $N_i$  and average sample mapping quality  $MQ_i$ . Among  
171 all 8550 repetitive and non-repetitive mismatch positions, the maximal probability of  
172 observing at least 5 “edited” reads was  $\sim 6.772e-15$  for a site with  $N = 13$  and average  
173  $MQ = 29$ . If Bonferroni correction is used then  $0.05 / 189,638 = 6.23e-07$  can be used as a  
174 threshold for transcriptome-wide significance, where 189,638 was the total number of  
175 queried cDNA positions with a sequencing depth of at least 5 cDNA reads that were at  
176 the location of homozygous loci in the genomic sequence. From this evidence we  
177 conclude that our pipeline sufficiently minimizes artifacts associated with mapping  
178 quality when using the *Sus scrofa* 10.2.69 assembly.



## 179 **Pig editome functional implications**

180 Little is known about the average effect of RNA editing transcriptome wide. For  
181 humans, one prevailing hypothesis is that the exonization of Alu SINE elements is  
182 controlled in part by A-to-G editing. An instance of this mechanism has been  
183 demonstrated, where intronic A-to-G editing events contribute to alternative splicing of  
184 *nuclear prelamins A* so that an Alu element is included in an exon [12]. To explore the  
185 possibility that RNA editing in pigs targets introns to affect splicing, editTools was used  
186 to synthesize mismatch data with Variant Effect Predictor data to find the relative  
187 locations of each mismatch relative to annotated transcripts. Consistent with what has  
188 been found in humans [2], nearly half of all detected A-to-G mismatches are located in  
189 retained introns (Fig. 4). The remaining sites are concentrated in other non-coding  
190 regions including 3' UTRs, intergenic, and gene proximal regions. While the majority of  
191 non-coding editing events in humans are attributed to the position and orientation of  
192 SINE elements within transcripts [10], coding RNA editing occurs rarely, usually outside  
193 repetitive elements but nevertheless site-specifically. It has been suggested that site-  
194 specificity of coding RNA editing events is facilitated by nearby SINE elements, which  
195 through their induction of long dsRNA regions, recruit ADAR in sufficient density to  
196 affect coding regions in close proximity [16]. From our data, only 49 pig A-to-G  
197 mismatches were found within coding regions and of those, 34 would result in a missense  
198 variant (Table 1). It can be noted that a number of amino acid changes resulting from  
199 verified macaque DNA RNA mismatches [8] can be found among our pig dataset –  
200 mismatches that control I/V in *COPA*, Y/C in *BLCAP*, I/V in *COG3*, K/R in *NEIL1*, and  
201 Q/R in *GRIA2*. Interestingly, Y/C recoding of *BLCAP* via RNA editing has been

202 associated with hepatocellular carcinoma (HCC) in humans as HCC samples were shown  
 203 to express edited *BLCAP* in significantly higher amounts than non-HCC samples [22].  
 204 Additionally, exon 6 K/R recoding of *NEILI* by RNA editing was previously thought to  
 205 be primate specific and attributed to the K/R site's proximity to Alu dense regions [23],  
 206 however we witness evidence of the same K/R recoding of exon 6 via an A-to-G editing  
 207 event in pigs. In fact SINE elements recruit ADAR to affect nearby coding regions,  
 208 then our data suggest the remarkable conservation of *NEILI* K/R recoding across  
 209 genomes with entirely different SINE elements.

210

211 **Table 1** A-to-G mismatches resulting in amino acid changes.

| Position    | Gene symbol/ID            | AA  | SIFT                        | Tissues      |
|-------------|---------------------------|-----|-----------------------------|--------------|
| 1:63408856  | <i>ENSSSCG00000029003</i> | L/P | tolerated(1)                | Fat LD Liver |
| 1:125424444 | <i>ENSSSCG00000024660</i> | Q/R | tolerated(1)                | Fat LD Liver |
| 2:12622576  | <i>LDHB</i>               | I/M | tolerated(1)                | Fat LD Liver |
| 2:49316285  | <i>ARNTL</i>              | K/E | tolerated low confidence(1) | Liver        |
| 4:98044799  | <i>COPA</i>               | I/V | deleterious(0.02)           | Fat          |
| 5:42375023  | <i>KRR1</i>               | I/T | deleterious(0.01)           | Liver        |
| 6:92516721  | <i>PTPRM</i>              | K/R | tolerated(1)                | Fat          |
| 6:146168578 | <i>NDC1</i>               | E/G | deleterious(0.01)           | Liver        |
| 7:62951442  | <i>NEILI</i>              | K/R | deleterious(0.02)           | Fat LD       |
| 7:81602273  | <i>ENSSSCG00000002045</i> | C/R | tolerated(1)                | Fat LD Liver |
| 7:102789222 | <i>ACOT4</i>              | T/A | tolerated(0.61)             | Fat          |
| 7:129322238 | <i>RPS21</i>              | C/R | -                           | Fat LD Liver |
| 8:28015971  | <i>ENSSSCG00000008767</i> | H/R | tolerated(1)                | Fat LD Liver |
| 8:31629014  | <i>TLR1</i>               | I/V | tolerated(1)                | Liver        |
| 8:32309809  | <i>RPL9</i>               | I/V | tolerated(0.4)              | Fat          |
| 8:32309814  | <i>RPL9</i>               | E/G | deleterious(0.01)           | Fat          |
| 8:48244993  | <i>GRIA2</i>              | Q/R | tolerated(0.07)             | Fat          |
| 9:41146365  | <i>ENSSSCG00000023913</i> | Q/R | deleterious(0.04)           | Fat          |
| 9:74510703  | <i>ENSSSCG00000015294</i> | K/R | tolerated(0.13)             | Liver        |

|              |                           |     |                                |              |
|--------------|---------------------------|-----|--------------------------------|--------------|
| 9:83273454   | <i>SLC25A13</i>           | E/G | deleterious(0.02)              | LD           |
| 11:22178068  | <i>COG3</i>               | I/V | tolerated(1)                   | Fat LD Liver |
| 12:20231860  | <i>AOC3</i>               | Q/R | tolerated(1)                   | Liver        |
| 13:131377159 | <i>EIF2B5</i>             | Q/R | tolerated(1)                   | Fat          |
| 13:156760971 | <i>UBE2B</i>              | D/G | tolerated(0.48)                | Fat LD Liver |
| 13:206979572 | <i>SON</i>                | R/G | -                              | Fat          |
| 14:40832826  | <i>PLBD2</i>              | R/G | tolerated low confidence(0.12) | Fat          |
| 14:52398588  | <i>IGLV-3</i>             | E/G | tolerated(0.05)                | Fat          |
| 14:59613334  | <i>LYST</i>               | S/G | -                              | LD           |
| 14:81796679  | <i>OIT3</i>               | S/G | tolerated(1)                   | Liver        |
| 15:59811585  | <i>HNRNPA2B1</i>          | L/P | tolerated(0.35)                | Fat LD Liver |
| 15:98217885  | <i>ENSSSCG00000028949</i> | R/G | tolerated low confidence(1)    | Fat LD Liver |
| 16:29335640  | <i>ENSSSCG00000016869</i> | N/D | tolerated(1)                   | Fat LD       |
| 16:42512978  | <i>ELOVL7</i>             | S/G | tolerated(1)                   | Fat          |
| 17:46041505  | <i>BLCAP</i>              | Y/C | deleterious(0)                 | Fat Liver    |

---

212

213

## 214 **Pig editome association with pig-specific SINE elements**

215         Since properties of the primate Alu element are suggested to influence RNA  
216 editing in both coding and non-coding regions, one of our primary interests was to  
217 determine which SINE elements in pigs are capable of attracting the majority of ADAR  
218 activity. Again using the functionality of editTools, we merged our mismatch data with  
219 data from RepeatMasker to determine which repetitive regions contain putative RNA  
220 editing sites. As mentioned previously, 5993 out of 6410 A-to-G mismatches are located  
221 within the body of a repetitive element. Upon closer inspection, 5715 of the 5993 are  
222 within pig SINE elements as opposed to LINE elements and others (Fig. 5A), although  
223 SINEs occupy just 11.4% of the swine genome, while LINEs occupy 17.5% [24]. Of the  
224 5993 repetitive A-to-G mismatches, 58.8% are found within the Pre0\_SS element, a

225 SINE element of the PRE1 family (Fig. 5B). Little is known about Pre0\_SS, but among  
226 all elements of the PRE1 family, Pre0\_SS is most identical to the consensus PRE1  
227 sequence. In many instances, Pre0\_SS elements are > 99% identical to one another,  
228 indicating that it is currently actively transposing in pigs [25]. Additional members of the  
229 PRE1 family contain A-to-G mismatches, although at a much lower frequency than  
230 Pre0\_SS.

231

## 232 **Conclusions**

233 While Alu elements enable substantial RNA editing among primate genomes, we  
234 show that non-Alu bearing genomes can also utilize RNA editing as a means to achieve a  
235 similar result. Our high-throughput scan suggests that pig transcriptomes are highly  
236 editable among PRE-1 SINE retrotransposons. PRE-1, an element derived from an  
237 ancestral tRNA, has similar features to the primate Alu, derived from an ancestral 7SL  
238 RNA; a copy number of  $1 \times 10^6$ , consensus length of 246bp, and very little diversity  
239 among such members as Pre0\_SS. These features influence the secondary structure of the  
240 transcriptome, which in turn affect ADAR editable targets. Surprisingly, conservation of  
241 specific editing sites such as those in *NEILI* and *BLCAP* appears evident between human  
242 and pigs. Therefore, we hypothesize that transcriptome secondary structure may be  
243 conserved among mammals enough to preserve particular RNA editing sites, and that  
244 SINE elements, regardless of origin, may conform to certain positions and orientations in  
245 order to allow conservation to occur.

246 By demonstrating that pig transcriptomes have potential to be highly edited, we  
247 propose that pigs may be a valuable model to understand the patterns of ADAR

248 controlled RNA editing. Additionally, by shedding light on the pig editome, we can begin  
249 to understand the extent to which this phenomenon enhances pig genetic variation. Such  
250 sources of variation may one day provide valuable explanatory power for a variety of  
251 traits of interest to both biomedical and agricultural communities.

252

## 253 **Methods**

### 254 **Sequence data**

255 From Michigan State University's pig resource population (MSUPRP), an F<sub>2</sub>  
256 population resulting from crosses between 4 F<sub>0</sub> Duroc sires and 15 F<sub>0</sub> Pietrain dams [26],  
257 a single female animal was chosen for whole genome and transcriptome sequencing.  
258 Total RNA was extracted from subcutaneous fat, liver, and LD skeletal muscle using  
259 TRIzol, and a RIN greater than 7 was determined with the Agilent 2100 Bioanalyzer.  
260 cDNA libraries were made using the Illumina TruSeq Stranded mRNA Library  
261 Preparation Kit. Sequencing was performed using the Illumina HiSeq 2500 in Rapid Run  
262 mode with 150x2 paired-end reads. Base calling was done by Illumina's Real Time  
263 Analysis v1.18.61 and the output was converted to FastQ format with Illumina's  
264 Bcl2fastq v1.8.4. Genomic DNA was purified from white blood cells using the Invitrogen  
265 Purelink Genomic DNA Mini Kit and libraries were made using the Illumina TruSeq  
266 Nano DNA Library Preparation Kit HT. Sequencing of genomic DNA was done using  
267 the Illumina HiSeq 2500 in Rapid Run mode with 150x2 paired-end reads. Real Time  
268 Analysis v.1.17.21.3 and Bcl2fastq v1.8.4 were used for base calling and FastQ

269 conversion, respectively. Read quality of both whole genome and RNA data was assessed  
270 using the FastQC program [27].

## 271 **Sequence preparation and mapping**

272 DNA reads from whole genome sequencing were trimmed for quality at the 3'  
273 end using Condetri v2.2 [28] with parameters: -sc=33 -minlen=75 and b=fq. Resulting  
274 mate 1, mate 2 and unpaired reads were mapped to *Sus Scrofa* 10.2.69 using Bowtie  
275 v2.2.1 [29] with parameters: -p 7 -X 1000. In order to filter out DNA reads that had more  
276 than one recorded alignment, alignments containing the “XS:i:<N>” tag, where N  
277 indicates the number of alternative alignments for a read, were removed. Strand specific  
278 cDNA sequencing reads from each tissue sample were trimmed with Condetri with  
279 parameters: -sc=33 -minlen=75 -pb=fq -cutfirst=6 -pb=fq. Resulting paired and unpaired  
280 cDNA reads were then mapped to *Sus Scrofa* 10.2.69 using TopHat v2.0.12 [30] with  
281 parameters: -p 7 --mate-inner-dist 400 --mate-std-dev 100 --library-type "fr-firststrand".  
282 Filtering out cDNA reads that had more than one recorded alignment was done by  
283 selecting alignments with the “NH:i:1” tag, while separating plus strand transcript  
284 alignments from minus strand alignments was done by selecting alignments possessing  
285 the “XS:A:” or “XS:A:-” tags, respectively. The resulting DNA and cDNA alignments  
286 are the “filtered” data used in downstream variant calling and mismatch detection.

## 287 **Variant calling and mismatch detection**

288 We utilized variant calling software Samtools v1.0 and Bcftools v1.2 to jointly  
289 call variants among DNA and cDNA reads from plus strand transcripts using: samtools  
290 mpileup -f <reference\_genome.fa> -C50 -E -Q25 -ug -t DP,DV,SP <DNA.bam>  
291 <liver\_plusstrand.bam> <fat\_plusstrand.bam> <LD\_plusstrand.bam>, where

292 <DNA.bam> includes all filtered DNA alignments, and <liver\_plusstrand.bam>, 293 <fat\_plusstrand.bam>, and <LD\_plusstrand.bam> are filtered cDNA alignments from 294 plus strand transcripts. Likewise, DNA and cDNA reads from minus strand transcripts 295 were processed similarly with: samtools mpileup -f <reference\_genome.fa> -C50 -E - 296 Q25 -ug -t DP,DV,SP <DNA.bam> <liver\_minusstrand.bam> <fat\_minusstrand.bam> 297 <LD\_minusstrand.bam>. Note that the parameter “-t DP,DV,SP” is required for 298 downstream mismatch detection with editTools. Samtools output from each command 299 was piped into bcftools with additional parameters: -O v -m -v. These steps produce two 300 VCF files that are simultaneously processed with find\_edits(), a function within editTools 301 available at <https://github.com/funkhou9/editTools>. By default, find\_edits() scans each 302 variant site to search for candidate RNA editing sites according to the five criteria 303 required for sufficient evidence (see Results and Discussion). Most figures in this report 304 were generated using editTools plotting methods, which utilized the ggplot2 R package 305 [31].

## 306 **Quantitative real-time PCR**

307 Total RNA was isolated from liver, LD skeletal muscle and subcutaneous fat 308 tissues from 34 MSUPRP pigs, including the pig chosen for sequencing, using TRIzol 309 reagent (Ambion) according to the manufacturer’s instructions. Concentrations were 310 measured using a NanoDrop spectrophotometer (Thermo Scientific), and quality and 311 integrity were determined using an Agilent 2100 Bioanalyzer (Agilent Technologies, 312 Inc.). Total RNA was reverse transcribed using random primers with the High Capacity 313 cDNA Reverse Transcription Kit with RNase Inhibitor (Applied Biosystems) according 314 to the manufacturer’s instructions. A pig ADAR Custom TaqMan Gene Expression assay

315 was designed using the online Custom TaqMan Assay Design Tool (ThermoFisher  
316 Scientific). The assay was designed to span exons 2-3 of the pig ADAR gene (Accession  
317 No. NC\_010446.4). Assays were performed in triplicate using 50 ng cDNA and the  
318 TaqMan Gene Expression Master Mix (20  $\mu$ l final volume per reaction) in a StepOnePlus  
319 Real-Time PCR System (Applied Biosystems). Cycling conditions were 52°C for 2 min  
320 and 95°C for 10 min, followed by 40 cycles of 95°C for 15 s and 60°C for 1 min.  
321 Relative expression values were obtained using the  $2^{-\Delta\Delta CT}$  method, with the muscle  
322 sample used for sequencing as a calibrator and Ubiquitin C as a reference gene (Applied  
323 Biosystems Assay No. Ss03374343\_g1). Inference of differential ADAR expression was  
324 calculated by one-way ANOVA (main effect of tissue on ADAR expression), and Tukey  
325 HSD (pairwise comparisons of tissue means).

## 326 **Calculating probability of mapping error**

327 The average phred-scaled mapping quality  $MQ$  across all samples at mismatch  
328 site  $i$  is provided by SAMTools output. From  $MQ$  we can compute the probability of  
329 mapping error  $p$  according to:

330

$$p_i = 10^{-\frac{MQ_i}{10}}$$

331

332 It follows that the probability of observing 5 “edited” reads at a homozygous site with a  
333 cDNA sequencing depth of  $N$  assuming no RNA editing can be modeled using the  
334 binomial distribution, where:

335



$$P(X \geq 5 | N, p) = 1 - P(X < 5) = 1 - \sum_{j=0}^4 \binom{N}{j} p^j (1-p)^{N-j}$$

## 336 **Incorporating RepeatMasker and Variant Effect Predictor**

### 337 **data using editTools**

338       The editTools function `add_repeatmask()` was used to merge a mismatch data  
339 object (generated with `find_edits()`) with `susScr3`, a Repeatmasker dataset available for  
340 download at: <http://www.repeatmasker.org/species/susScr.html>. This function utilizes a  
341 binary search algorithm implemented in C++ to process large RepeatMasker files  
342 efficiently. The function `write_vep()` was used to generate Variant Effect Predictor input  
343 from a mismatch data object. The output of Variant Effect Predictor was merged with the  
344 mismatch data object using `add_vep()`. Additional documentation for `find_edits()`,  
345 `write_vep()`, `add_vep()`, `add_repeatmask()` is available within editTools v2.1.

346

## 347 **Abbreviations**

348 **ADAR:** adenosine deaminase acting on RNA

349 **LD:** *longissimus dorsi*

350 **LINE:** long interspersed nuclear element

351 **SINE:** short interspersed nuclear element

352 **UTR:** untranslated region

353

## 354 **Declarations**

### 355 **Ethics approval and consent to participate**

356 Animal protocols were approved by the Michigan State University All University  
357 Committee on Animal Use and Care (AUF# 09/03-114-00).

### 358 **Consent for publication**

359 Not applicable

### 360 **Availability of data and materials**

361 Raw whole genome sequencing and RNA-seq data are accessible from the Sequence  
362 Read Archive, BioProject PRJNA354435.

### 363 **Competing interests**

364 The authors declare that they have no competing interests.

### 365 **Funding**

366 This project is supported by Agriculture and Food Research Initiative Competitive Grant  
367 no. 2014-67015-21619 from the USDA National Institute of Food and Agriculture, and  
368 by MSU AgBioResearch and the College of Natural Science at Michigan State  
369 University. The funders had no role in study design, data collection and analysis, decision  
370 to publish, or preparation of the manuscript.

### 371 **Authors' contributions**

372 Conceived and designed the study: CWE. Contributed samples from the MSU pig  
373 resource population: ROB, CWE, NER. Isolated RNA and DNA: NER. Developed

374 software and analysis pipeline: SAF, JPS. Performed qPCR assays and analysis: DS,  
375 NER, SAF. Wrote the manuscript: SAF. All authors read and approved the final  
376 manuscript.

## 377 **Acknowledgements**

378 Computing resources were provided by Michigan State University's High Performance  
379 Computing Cluster. Sequencing was performed at the Michigan State University  
380 Research Technology Support Facility.

381

382

## 383 **References**

- 384 1. Benne R, Van Den Burg J, Brakenhoff JPJ, Sloof P, Van Boom JH, Tromp MC. Major  
385 transcript of the frameshifted coxII gene from trypanosome mitochondria contains four  
386 nucleotides that are not encoded in the DNA. *Cell*. 1986;46: 819–26.
- 387 2. Athanasiadis A, Rich A, Maas S. Widespread A-to-I RNA editing of Alu-containing  
388 mRNAs in the human transcriptome. *PLoS Biol*. 2004;2: e391.
- 389 3. Blow M. A survey of RNA editing in human brain. *Genome Res*. 2004;14: 2379–87.
- 390 4. Levanon EY, Eisenberg E, Yelin R, Nemzer S, Hallegger M, Shemesh R, et al.  
391 Systematic identification of abundant A-to-I editing sites in the human transcriptome.  
392 *Nat Biotechnol*. 2004;22: 1001–5.
- 393 5. Eisenberg E, Nemzer S, Yaron K, Rotem S, Gideon R, Levanon EY. Is abundant A-to-  
394 I RNA editing primate-specific? *Trends Genet*. 2005;21: 73–7.
- 395 6. Neeman Y. RNA editing level in the mouse is determined by the genomic repeat  
396 repertoire. *RNA*. 2006;12: 1802–9.
- 397 7. Bazak L, Haviv A, Barak M, Jacob-Hirsch J, Deng P, Zhang R, et al. A-to-I RNA  
398 editing occurs at over a hundred million genomic sites, located in a majority of human  
399 genes. *Genome Res*. 2014;24: 365–76.
- 400 8. Chen J-Y, Peng Z, Zhang R, Yang X-Z, Tan BC-M, Fang H, et al. RNA editome in  
401 Rhesus Macaque shaped by purifying selection. *PLoS Genet*. 2014;10: e1004274.

- 402 9. Lander ES, Linton LM, Birren B, Nusbaum C, Zody MC, Baldwin J, et al. Initial  
403 sequencing and analysis of the human genome. *Nature*. 2001;409: 860–921.
- 404 10. Bazak L, Levanon EY, Eisenberg E. Genome-wide analysis of Alu editability.  
405 *Nucleic Acids Res*. 2014;42: 6876–84.
- 406 11. Vassetzky NS, Kramerov DA. SINEBase: a database and tool for SINE analysis.  
407 *Nucleic Acids Res*. 2013;41: D83–D89.
- 408 12. Lev-Maor G, Sorek R, Levanon EY, Paz N, Eisenberg E, Ast G. RNA-editing-  
409 mediated exon evolution. *Genome Biol*. 2007;8: R29.
- 410 13. Scadden ADJ, Smith CWJ. RNAi is antagonized by A→I hyper-editing. *EMBO Rep*.  
411 2001;2: 1107–11.
- 412 14. Kleinman CL, Adoue V, Majewski J. RNA editing of protein sequences: A rare event  
413 in human transcriptomes. *RNA*. 2012;18: 1586–96.
- 414 15. Higuchi M, Maas S, Single FN, Hartner J, Rozov A, Burnashev N, et al. Point  
415 mutation in an AMPA receptor gene rescues lethality in mice deficient in the RNA-  
416 editing enzyme ADAR2. *Nature*. 2000;406: 78–81.
- 417 16. Ramaswami G, Lin W, Piskol R, Tan MH, Davis C, Li JB. Accurate identification of  
418 human Alu and non-Alu RNA editing sites. *Nat Methods*. 2012;9: 579–81.

- 419 17. Lin W, Piskol R, Tan MH, Li JB. Comment on “Widespread RNA and DNA  
420 sequence differences in the human transcriptome.” *Science*. 2012;335: 1302; author  
421 reply 1302.
- 422 18. Li H. A statistical framework for SNP calling, mutation discovery, association  
423 mapping and population genetical parameter estimation from sequencing data.  
424 *Bioinformatics*. 2011;27: 2987–93.
- 425 19. Deffit SN, Hundley HA. To edit or not to edit: regulation of ADAR editing specificity  
426 and efficiency. *Wiley Interdiscip Rev RNA*. 2015;7.
- 427 20. Pickrell JK, Gilad Y, Pritchard JK. Comment on “Widespread RNA and DNA  
428 sequence differences in the human transcriptome”. *Science*. 2012;335: 1302; author  
429 reply 1302.
- 430 21. Li H, Ruan J, Durbin R. Mapping short DNA sequencing reads and calling variants  
431 using mapping quality scores. *Genome Res*. 2008;18: 1851–8.
- 432 22. Hu X, Wan S, Ou Y, Zhou B, Zhu J, Yi X, et al. RNA over-editing of BLCAP  
433 contributes to hepatocarcinogenesis identified by whole-genome and transcriptome  
434 sequencing. *Cancer Lett*. 2015;357: 510–519.
- 435 23. Daniel C, Silberberg G, Behm M, Öhman M. Alu elements shape the primate  
436 transcriptome by cis-regulation of RNA editing. *Genome Biol*. 2014;15: R28.
- 437 24. Smit AFA, Hubley R, Green P. 2013. RepeatMasker Open-4.0. 2013-2015.  
438 Available: <http://www.repeatmasker.org>

- 439 25. Jurka J, Kapitonov VV, Pavlicek A, Klonowski P, Kohany O, Walichiewicz J.  
440 Repbase Update, a database of eukaryotic repetitive elements. *Cytogenet Genome*  
441 *Res.* 2005;110: 462–7.
- 442 26. Edwards DB, Ernst CW, Tempelman RJ, Rosa GJ, Raney NE, Hoge MD, Bates RO.  
443 Quantitative trait loci mapping in an F2 Duroc x Pietrain resource population: I.  
444 Growth traits. *J Anim Sci.* 2008;86: 241-53.
- 445 27. Andrews S. 2010. FastQC: a quality control tool for high throughput sequence data.  
446 Available: <http://www.bioinformatics.babraham.ac.uk/projects/fastqc>
- 447 28. Smeds L, Künstner A. ConDeTri - A content dependent read trimmer for Illumina  
448 data. *PLoS One.* 2011;6: e26314.
- 449 29. Langmead B, Salzberg SL. Fast gapped-read alignment with Bowtie 2. *Nat Methods.*  
450 2012;9: 357–9.
- 451 30. Trapnell C, Pachter L, Salzberg SL. TopHat: discovering splice junctions with RNA-  
452 Seq. *Bioinformatics.* 2009;25: 1105–11.
- 453 31. Wickham H. *ggplot2: elegant graphics for data analysis.* Springer-Verlag New York;  
454 2009.
- 455
- 456
- 457
- 458

## 459 **Figures**

460 **Fig. 1.** DNA to RNA mismatch counts. Comparing all mismatches found transcriptome  
461 wide (Left) to those within the body of a repetitive element (Right). Percentages shown  
462 are out of all mismatches found in each category.

463

464 **Fig. 2.** Shared A-to-G mismatches between tissues. A mismatch between two or more  
465 tissues was considered shared if it occurred at the same physical position and on the same  
466 strand.

467

468 **Fig. 3.** Relative ADAR transcript abundance between tissues. Expression was measured  
469 relative to the LD muscle sample used for sequencing. Using a one-way ANOVA, a  
470 significant effect of tissue on ADAR expression was detected ( $p < 0.0001$ ). Pairwise  
471 comparisons of tissue means using Tukey HSD shows significant differences in ADAR  
472 expression between LD and liver ( $p < 0.00001$ ) and between LD and fat ( $p < 0.003$ ), but  
473 no significant difference between fat and liver ( $p = 0.0505563$ ).

474

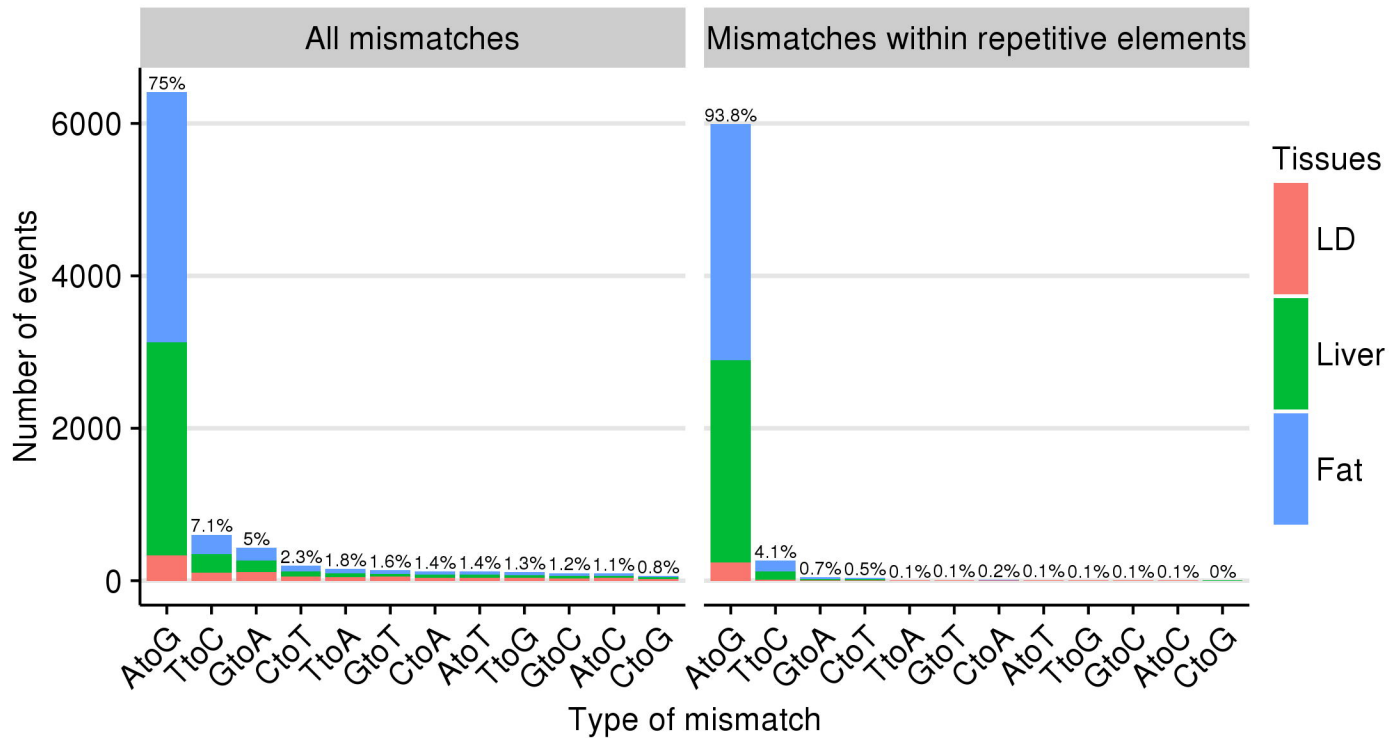
475 **Fig. 4.** A-to-G mismatch locations relative to the nearest annotated gene. Percentages  
476 shown are out of all A-to-G mismatches.

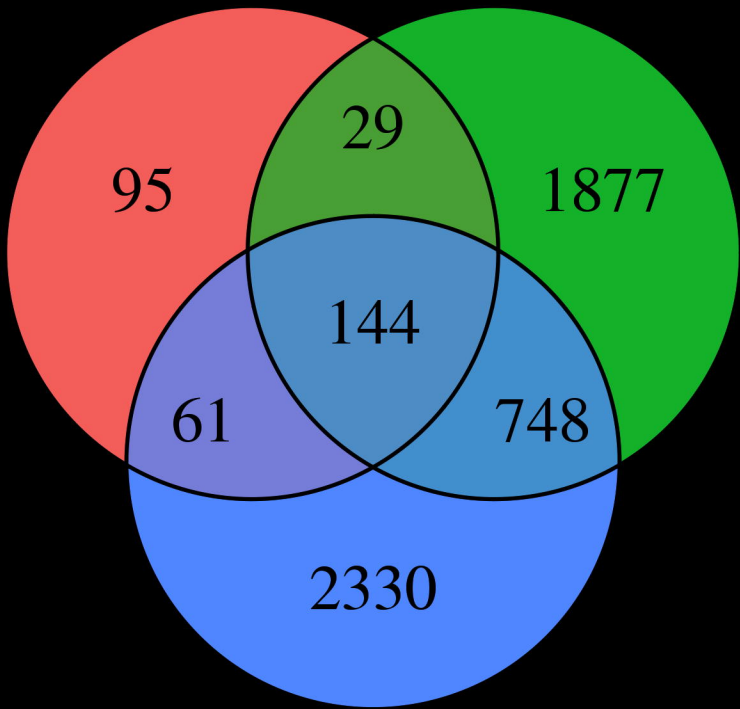
477

478 **Fig. 5.** Distribution of repetitive A-to-G mismatches. The distribution is shown across  
479 major repetitive element families (A) and further broken down into specific repetitive  
480 element types (B). Percentages shown are out of all repetitive A-to-G mismatches.

481







Fold-change in expression

bioRxiv preprint doi: <https://doi.org/10.1101/096321>; this version posted January 5, 2017. The copyright holder for this preprint (which was not certified by peer review) is the author/funder, who has granted bioRxiv a license to display the preprint in perpetuity. It is made available under aCC-BY-NC-ND 4.0 International license.

300  
200  
100  
0

muscle

liver  
Tissue

fat

